



## OPEN Nose-to-brain delivery of human muse cells enhances structural and functional recovery in the murine ischemic stroke model

Shusuke Yamamoto<sup>1✉</sup>, Keitaro Shiraishi<sup>1</sup>, Yoshihiro Kushida<sup>2</sup>, Yo Oguma<sup>2</sup>, Shohei Wakao<sup>2</sup>, Mari Dezawa<sup>2✉</sup> & Satoshi Kuroda<sup>1✉</sup>

Muse cells are endogenous, non-tumorigenic, pluripotent-like stem cells already applied to clinical trials based on intravenous injection. They can selectively home to the post-infarct area, replenish apoptotic neural cells by phagocytosis-induced differentiation, and enhance functional recovery. The effect of nose-to-brain delivery of Muse cells on cerebral infarct was examined. Permanent middle cerebral artery occlusion model BALB/c mice received intranasal administration of either human Muse cells ( $6.0 \times 10^4$  cells), high-dose human-mesenchymal stem cells (MSCs) ( $1.6 \times 10^6$  cells), low-dose human-MSCs ( $6.0 \times 10^4$  cells), or vehicle at 7 days after onset. An accelerated rotarod test and a histological assessment were done. The vehicle- or low-dose MSC groups showed no significant improvement in the rotarod test. In the high-dose MSC group, motor function was transiently recovered, but the therapeutic effect disappeared thereafter. The Muse group continuously improved motor function, with statistical significance to the other groups. The engraftment of administered cells in the peri-infarct area was the highest in the Muse group, while few cells were detected in other groups.  $63.6 \pm 8.5\%$  and  $26.2 \pm 3.0\%$  of Muse cells were positive for NeuN and GSTpi, respectively. Intranasal administration of Muse cells might be a viable approach to improving functional recovery with less invasiveness after ischemic stroke.

**Keywords** Ischemic stroke, Muse cell, Mesenchymal stem cell, Intranasal administration

### Abbreviations

|               |  |
|---------------|--|
| $\alpha$ -MEM | $\alpha$ -Minimum essential medium           |
| ANOVA         | Analysis of variance                         |
| BDNF          | Brain-derived neurotrophic factor            |
| BMSC          | Bone marrow stromal cell                     |
| BSA           | Bovine serum albumin                         |
| CXCR4         | C-X-C chemokine receptor type 4              |
| DAPI          | 4',6-diamidino-2-phenylindole                |
| FACS          | Fluorescence-activated cell sorting          |
| FAK           | Focal adhesion kinase                        |
| FBS           | Fetal bovine serum                           |
| FITC          | Fluorescein isothiocyanate                   |
| GFAP          | Glial fibrillary acidic protein              |
| GSTpi         | Glutathione S-transferase-pi                 |
| HLA           | Human leukocyte antigen                      |
| MAP           | Microtubule-associated protein               |
| MCAO          | Middle cerebral artery occlusion             |
| MSC           | Mesenchymal stem cell                        |
| Muse          | Multilineage-differentiating stress-enduring |
| NGF           | Nerve growth factor                          |

<sup>1</sup>Department of Neurosurgery, Graduate School of Medicine and Pharmaceutical Science, University of Toyama, 2630 Sugitani, Toyama 930-0194, Japan. <sup>2</sup>Department of Stem Cell Biology and Histology, Tohoku University Graduate School of Medicine, Sendai, Japan. ✉email: shuyama@med.u-toyama.ac.jp; mari.dezawa.e1@tohoku.ac.jp; skuroda@med.u-toyama.ac.jp

|                |  |
|----------------|--|
| PBS            | Phosphate-buffered saline              |
| SD             | Standard deviation                     |
| SDF-1 $\alpha$ | Stromal cell-derived factor-1 $\alpha$ |
| SSEA           | Stage specific embryonic antigen       |
| VEGF           | Vascular endothelial growth factor     |

Ischemic stroke can cause various functional impairments. Although acute reperfusion therapies such as intravenous injection of tissue-type plasminogen activator and mechanical thrombectomy have been widely performed recently<sup>1</sup>, many stroke survivors are still forced to live with disabling conditions. Therefore, cell therapy has been expected to promote functional recovery after ischemic stroke for these three decades. Of many candidates for donor cells, mesenchymal stem cells (MSCs) have been subjected to clinical studies because they are easily accessible, non-tumorigenic, and do not involve ethical or immunological problems<sup>2</sup>. MSC transplantation has been suggested to provide some therapeutic effects in non-human and human studies. However, the phenotypic change of MSCs into functional cells in the post-infarct tissue has yet to be demonstrated, and the primary mechanism of action is considered trophic factor secretion<sup>3</sup>. Furthermore, there are still several issues to be resolved, including their poor homing ability, low survival rate, and unreliable effectiveness in the long term<sup>4</sup>.

Multilineage-differentiating stress-enduring (Muse) cells are endogenous non-tumorigenic pluripotent-like/macrophage-like stem cells that are distributed in the bone marrow, peripheral blood, organ connective tissues, and umbilical cord as stage-specific embryonic antigen (SSEA)-3-positive cells and are stress tolerant<sup>5–8</sup>. Muse cells can self-renew and differentiate into triploblastic lineages at a single-cell level, similar to pluripotent stem cells, while on the other hand, they exhibit low telomerase activity and do not form tumors when transplanted in vivo<sup>5,8,9</sup>. Muse cells sense sphingosine-1-P (S1P), the universal damage signal produced by damaged cells, and selectively migrate to and home to the damaged tissue rather than being trapped in the lung capillaries<sup>10</sup>. After homing to the damaged tissue, Muse cells phagocytose damaged/apoptotic cells, directly recycle signals from the up-taken damaged/apoptotic cells necessary for differentiation, such as transcription factors, and quickly differentiate into the same cell type as the phagocytosed damaged/apoptotic cells<sup>11</sup>. In addition, human leukocyte antigen (HLA)-mismatch allogeneic Muse cells escape immune rejection and survive in the host tissue over the long term without immunosuppressant treatment; this characteristic may be partly explained by Muse cell expression of HLA-G, which contributes to the immune privilege of the placenta<sup>10,12</sup>. Because of these characteristics, HLA-mismatch allogeneic-Muse cells can be directly administered intravenously without immunosuppressant, the Muse cell treatment does not require gene introduction to render pluripotency or to differentiate into target cell types before use. Indeed, intravenous or direct injection of Muse cells into the middle cerebral artery occlusion (MCAO) or lacunar infarction rodents showed the enhancement of functional recovery by differentiating into neural cells in the peri-infarct area<sup>13,14</sup>. Clinical trials conducted by intravenous administration of donor-Muse cells without HLA-matching or long-term immunosuppressant treatment in myocardial infarction<sup>15</sup>, epidermolysis bullosa<sup>16</sup>, subacute stroke<sup>17</sup>, amyotrophic lateral sclerosis<sup>18</sup>, neonatal hypoxic-ischemic encephalopathy<sup>19</sup>, and spinal cord injury<sup>20</sup> demonstrated safety and therapeutic efficacy.

Various routes have been proposed for cell therapy. For instance, direct injection for cerebral infarction requires craniotomy or burr hole surgery, and thus an injection may damage brain tissue<sup>13,21</sup>. Intra-arterial injection may have a risk of harmful embolism<sup>22</sup>. Intravenous injection may result in low homing rates to the brain<sup>4,23–28</sup>. In contrast, intranasal administration offers a non-invasive straightforward approach compared to other delivery methods described above. This non-invasiveness of intranasal administration is a crucial advantage because cells do not pass through the lungs and other organs, going directly into the brain through the cribriform plate<sup>29–32</sup>. Notably, previous reports have shown promising results with intranasally delivered MSCs in rodent stroke models; administered MSCs could reduce the infarct volume, decrease the number of apoptotic cells in the peri-infarct area, and promote sensorimotor functional recovery<sup>31,33</sup>.

In this study, we aimed to evaluate the efficacy of intranasal administration of Muse cells in the ischemic stroke model mice.

## Methods

All animal experiments were approved by the Animal Study Ethical Committee of the University of Toyama (A2021MED-22). All methods were performed in accordance with the relevant guidelines and regulations. All methods are reported in accordance with ARRIVE guidelines for the reporting of animal experiments.

### Mice permanent MCAO model

Male 8-week-old BALB/c mice were purchased from CLEA Japan, Inc. (Tokyo, Japan). Permanent MCAO was induced as described previously with minor modifications<sup>13,34</sup>. Briefly, anesthesia was induced with 5.0% sevoflurane in N<sub>2</sub>O: O<sub>2</sub> (70:30) and maintained with 3.0% sevoflurane in N<sub>2</sub>O: O<sub>2</sub> (70:30). A 1.0-cm vertical skin incision was made between the right eye and ear, and the temporal muscle was mobilized. Under a surgical microscope, a small craniotomy was created using a small dental drill. The dura mater was kept intact, and the right MCA was ligated using a 10–0 nylon thread through the dura mater. Only animals that circle towards the paretic side were included in this study.

### Preparation of human-Muse cells and -MSCs

Human bone marrow-MSCs (h-MSCs) were purchased from Lonza (Basel, Switzerland, PT-2501). Cells were maintained in culture medium comprising  $\alpha$ -minimum essential medium ( $\alpha$ -MEM, MilliporeSigma, St Louis, Mo, USA) with 10% (vol/vol) fetal bovine serum (FBS, HyClone, Logan, UT, USA), 1 ng/mL basic fibroblast growth factor (Milenyi Biotec, Bergisch Gladbach, Germany), 2 mM GlutaMAX I (ThermoFisher Scientific,

Waltham, MA, USA), and 0.1 mg/mL kanamycin sulfate (ThermoFisher Scientific) at 37 °C in 95% air and 5% CO<sub>2</sub>. To collect Muse cells, h-MSCs were incubated with anti-SSEA-3 antibody (1:1000, #330302; BioLegend, San Diego, CA, USA) and stained with secondary antibody, fluorescein isothiocyanate (FITC)-conjugated anti-rat IgM (1:100; Jackson ImmunoResearch, West Grove, PA, USA; 112-095-075), as previously described<sup>35</sup>. Human-Muse cells were then collected as SSEA-3(+) fractions by fluorescence-activated cell sorting (FACS; BD FACS Aria™ II cell sorter, BD Biosciences [BD], San Jose, CA, USA).

### Nose-to-brain cell administration

The animals were separated into four groups: Muse cell, high-dose MSC, low-dose MSC, and vehicle groups ( $n = 10$  in each group). Seven days after MCAO and 30 min before cell administration, each mouse received a total of 10- $\mu$ L (10 mg/mL) hyaluronidase (Sigma, St. Louis, MO; dissolved in sterile phosphate-buffered saline (PBS)) delivered into the nasal cavity (5  $\mu$ L in each nostril). Hyaluronidase increases tissue permeability of the nasopharyngeal mucosa, facilitating the invasion of stem cells into the brain<sup>29,31,33</sup>. One set of animals was randomly designated as the vehicle group receiving PBS (100  $\mu$ L), and the other set was given either of Muse cells ( $6.0 \times 10^4$  cells/100  $\mu$ L), high-dose MSCs ( $1.6 \times 10^6$  cells/100  $\mu$ L), or low-dose MSCs ( $6.0 \times 10^4$  cells/100  $\mu$ L). Because the proportion of Muse cells in bone marrow MSCs is several percent<sup>5–8</sup>, the high-dose MSCs include almost the same number of Muse cells as the Muse group<sup>5</sup>. A 5- $\mu$ L drop containing the cell suspension or vehicle was carefully placed on one nostril, alternating the nostrils with 1-minute intervals.

### Motor function test

The animals' motor function was serially assessed before and at 1, 7, 14, 21, 28, 42, 56, 70, and 84 days after the onset of ischemia, using a Rotarod treadmill. This behavioral test was performed in all the vehicle-, low-dose MSC-, high-dose MSC-, and Muse cell-treated mice. The Rotarod was set to the acceleration mode from 4 to 40 rpm for 5 min. The maximum time the animal stayed on the Rotarod was recorded for each performance<sup>13</sup>.

### Histological analysis

At 84 days after the onset of ischemia, the animals were deeply anesthetized with 5.0% sevoflurane in N<sub>2</sub>O: O<sub>2</sub> (70:30) and transcardially perfused with 4% paraformaldehyde (PFA) in PBS. The brain was removed, immersed in 4% PFA in PBS for another two days, and 20- $\mu$ m-thick coronal cryosections were made at 4 mm, 2.8 mm, 2 mm, and 1 mm anterior and 0.25 mm, 0.75 mm, 1.4 mm, and 2.2 mm posterior to bregma. To detect and the injected human Muse cells, frozen sections were washed with PBS, incubated with 20% Block-Ace (KAC Co.; Kyoto, Japan)/5% bovine serum albumin (BSA, Nacalai Tesque, Kyoto, Japan)/0.3% Triton X-100 in PBS solution for blocking, incubated with rabbit anti-human mitochondria antibody (1:200; abcam, ab 133789) diluted with 5% Block-Ace/1% BSA/0.3% Triton X-100/PBS solution, followed by incubation with secondary antibody of Alexa Fluor 488-conjugated donkey anti-rabbit IgG antibody (1:200; Jackson ImmunoResearch, 711-546-152). When evaluating the differentiation of administered cells in the mouse brain, the sections were washed with PBS and incubated with either mouse anti-NeuN (a marker for neurons; 1:200; MilliporeSigma, MAB377), goat anti-glutathione S-transferase (GST)pi (a marker for oligodendrocytes<sup>36</sup>; 1:500; abcam, ab53943), or mouse anti-gial fibrillary acidic protein (GFAP) antibodies (a marker for astrocytes; 1:500; MilliporeSigma, G3893), followed by incubation with secondary antibody of either Alexa Fluor 594-conjugated donkey anti-mouse IgG antibody (1:200; Jackson ImmunoResearch, 715-586-150) or Alexa Fluor 594-conjugated donkey anti-goat IgG antibody (1:200; Jackson ImmunoResearch, 705-586-147). The sections were counterstained by 4',6-diamidino-2-phenylindole (DAPI; 1:500; Thermo Fisher Scientific, D1306). Images were acquired with a confocal laser microscope (A1; Nikon, Tokyo, Japan). Cells double-positive for human mitochondria, and either NeuN, GSTpi, or GFAP were quantified using ImageJ.1.53t and calculated from whole brain images in each section.

### Statistical analysis

The data were collected and analyzed in a blind manner. All data were expressed as mean  $\pm$  standard deviation (SD). Continuous data were compared by one-factor analysis of variance (ANOVA) followed by Tukey-Kramer honestly significant difference test among four groups. Values of  $P < 0.05$  were considered statistically significant.

## Results

### Effect of nose-to-brain cell administration on motor function recovery

Forty-eight mice were induced MCAO. Among them, 40 circled towards the paretic side, which were included in this experiment. Figure 1 shows the results of the accelerated Rotarod test. In all animals ( $N = 40$ ), motor function significantly worsened up to 24–33% and 24–32% of the controls at one day and 7 days after the onset, respectively. There was no significant difference in motor function among 4 groups at this time point. The vehicle group showed no significant improvement in motor function throughout the experimental time. Likewise, the low-dose MSC group showed no significant improvement in motor function after cell administration. The high-dose MSC group showed a significant functional recovery at 14 days, compared to pre-treatment timing ( $P < 0.05$ ), while the therapeutic effect was lost thereafter. On the other hand, the motor function in the Muse group showed continuous improvement and demonstrated significant recovery compared to pre-treatment timing from 21 days after cell administration ( $P < 0.01$  at each time point). The therapeutic effects were observed thereafter.

As shown in Fig. 2, one-factor ANOVA demonstrated significant differences in motor function between the vehicle and Muse groups at 21, 35, 49, 63, and 77 days ( $P < 0.05$ ,  $P < 0.01$ ,  $P < 0.01$ ,  $P < 0.01$ , and  $P < 0.01$ , respectively). There were significant differences in motor function between the low-dose MSC and Muse groups at 35, 49, 63, and 77 days ( $P < 0.05$ ,  $P < 0.05$ ,  $P < 0.01$ , and  $P < 0.01$ , respectively). Likewise, a significant difference in motor function between the high-dose MSC and Muse groups at 77 days ( $P < 0.05$ ).

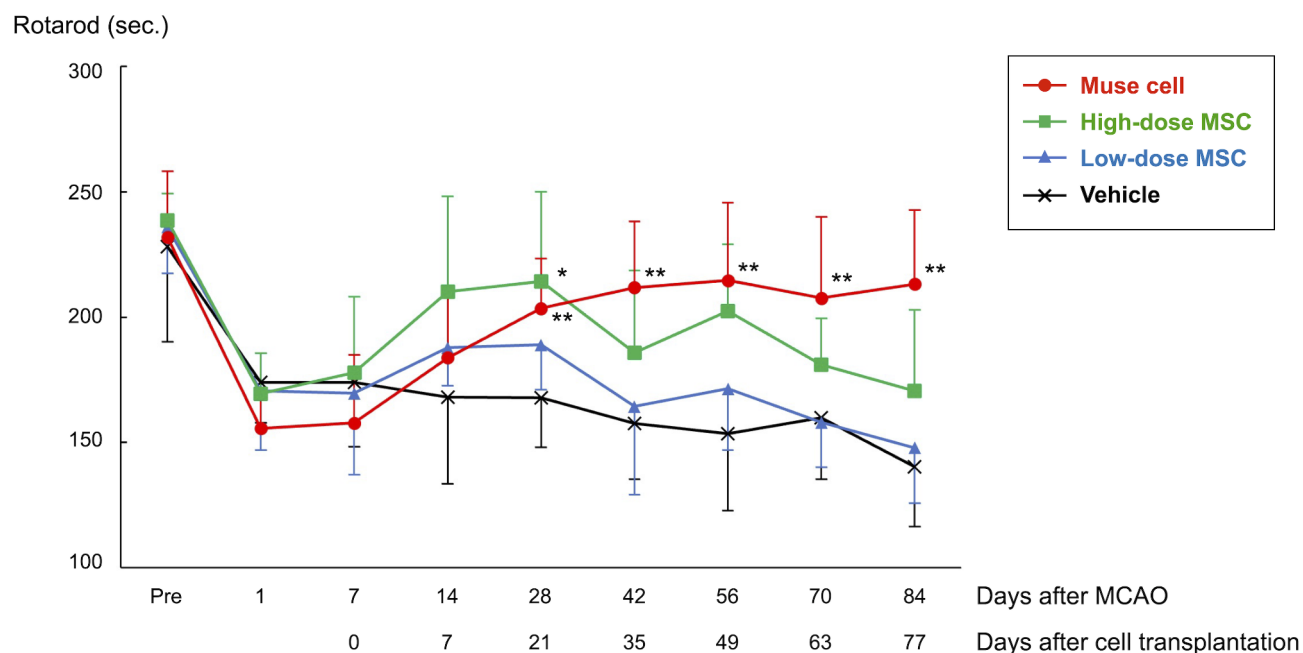


**Fig. 1.** Rotarod treadmill performance. A line graph shows the temporal profile of functional recovery in Muse cell- (red), high-dose MSC- (green), low-dose MSC- (blue), and vehicle-treated mice (black) subjected to permanent middle cerebral artery occlusion. \*,  $P < 0.05$ ; \*\*,  $P < 0.01$  vs. pretreatment.

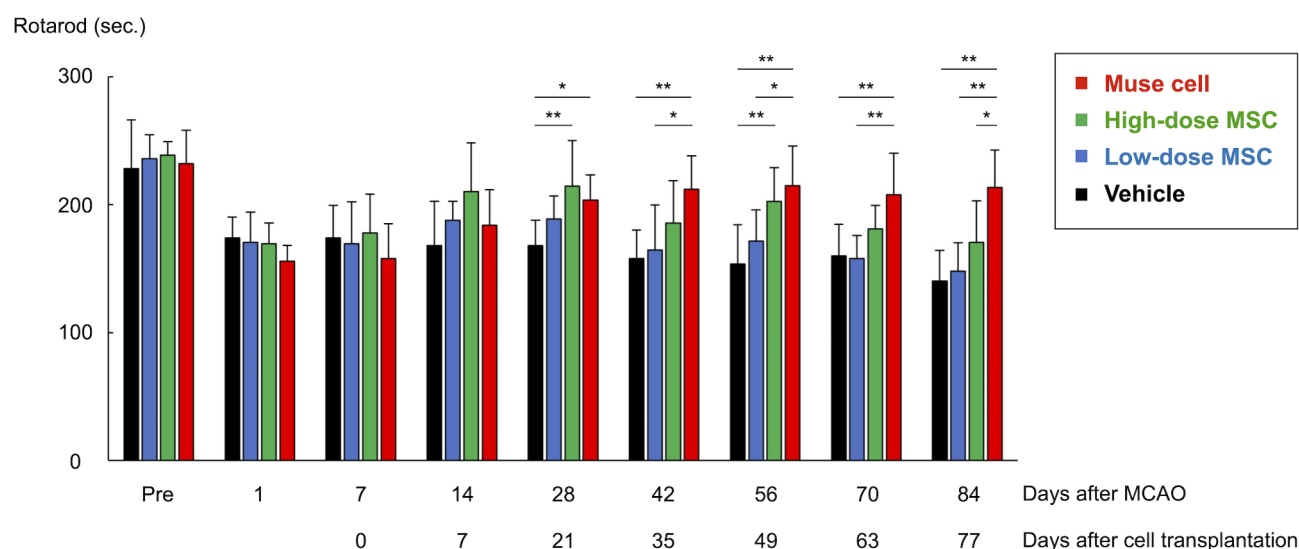


**Fig. 2.** Effects of cell therapy with vehicle, low-dose MSCs, high-dose MSCs, and Muse cells on motor dysfunction. A bar graph shows the Rotarod treadmill performance in Muse cell- (red), high-dose MSC- (green), low-dose MSC- (blue), and vehicle-treated mice (black), respectively. \*,  $P < 0.05$ ; \*\*,  $P < 0.01$ .

### Distribution and marker expression of muse cells after homing to the brain

Using anti-human mitochondria antibodies, human Muse cells and MSCs were detected in the mouse brain in immunohistochemical analysis. In the Muse group, human mitochondria (+) cells were mainly distributed in the ipsilateral side of the brain, most intensively in the peri-infarct area (Fig. 3A, B). In contrast, very few numbers of human mitochondria (+) MSCs were detected in the low- and high-dose MSC groups (Fig. 3B). No human mitochondria (+) cells were observed in the vehicle group (Fig. 3B). As shown in Fig. 3C, the number of human mitochondria (+) cells was significantly greater in the Muse cells group than in the low- and high-dose MSC groups in the slices at +3 to -2 mm from the bregma.

Then, multi-color fluorescence immunofluorescence was conducted to characterize the phenotype of the mitochondria-positive cells in the host brain of the Muse group. As a result,  $63.6 \pm 8.5\%$  and  $26.2 \pm 3.0\%$  of human

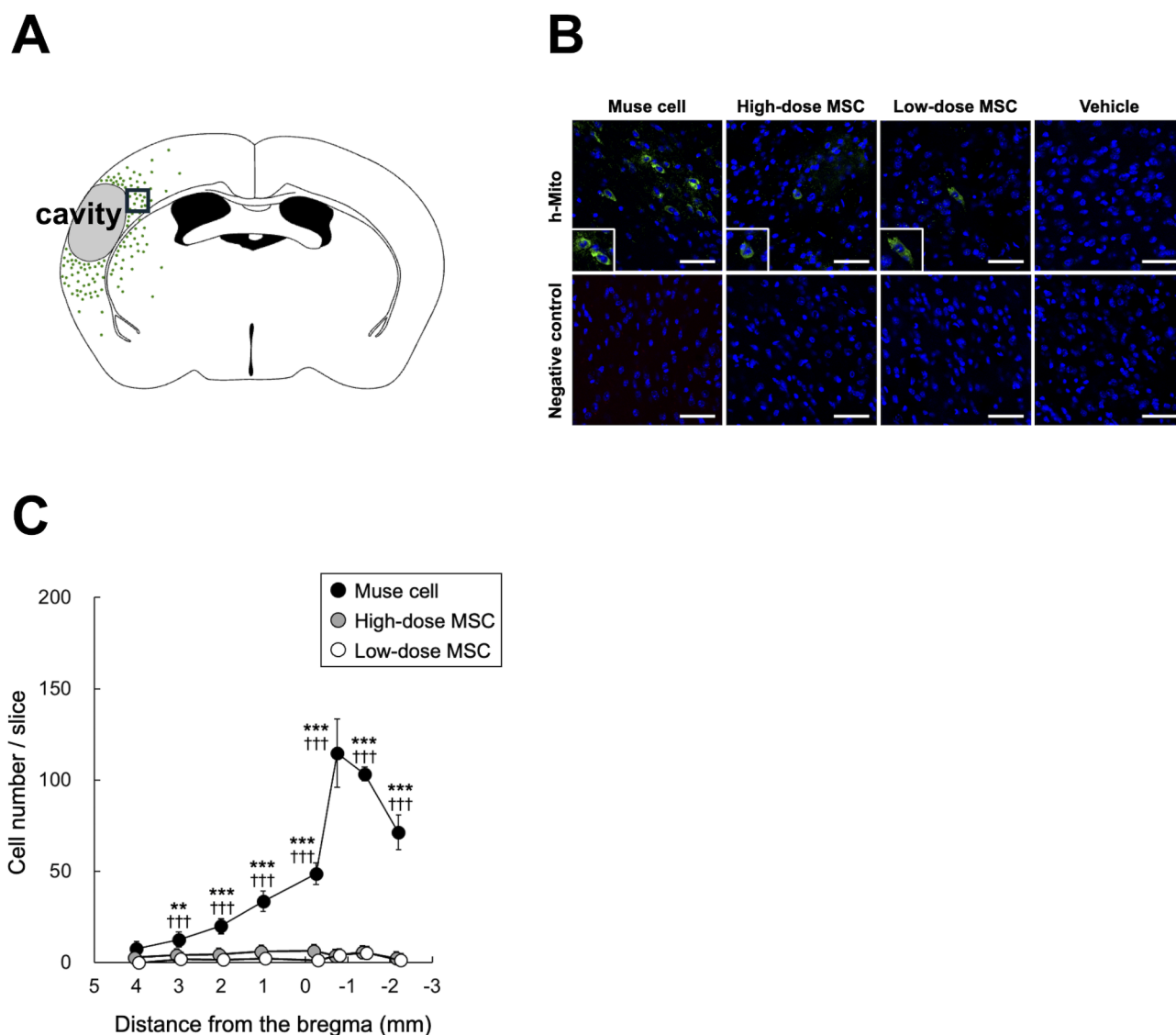


**Fig. 3.** Fluorescent staining for detecting human mitochondria-positive cells. (A) A diagram demonstrates the distribution of human mitochondria-positive cells. Green plots represent the human mitochondria-positive cells in the brain. The engrafted cells are densely distributed in the peri-infarct area. The black square indicates the location of magnified fluorescence immunohistochemistry images shown in Panel B. (B) On fluorescence immunohistochemistry for the muse brain harvested at 84 days after the onset of ischemia, the human mitochondria-positive cells were found in the Muse group, but were very sparse in the high-dose and low-dose MSC groups. None of them were observed in the vehicle group. (C) Semi-quantitative analysis of engrafted cells in the infarct brain harvested at 84 days after the onset of ischemia. A line graph shows the number of human mitochondria-positive cells per slice in Muse cell- (black circles), high-dose MSC- (gray circles), and low-dose MSC-treated mice (white circles) subjected to permanent middle cerebral artery occlusion, respectively. \*\* and \*\*\*,  $P < 0.01$  and  $P < 0.001$ , Muse group vs. high-dose MSC group; †††,  $P < 0.001$ , Muse group vs. low-dose MSC group.

mitochondria-positive cells were double positive for NeuN, a neuronal marker, and GSTpi, an oligodendrocyte marker, respectively. On the other hand, no human mitochondria-positive cells co-expressed the astrocytic marker, GFAP, in the Muse group brain (Fig. 4).

## Discussion

This is the first study investigating the therapeutic effects of intranasal administration of human Muse cells in ischemic stroke model mice. As a result, transnasally administered Muse cells continuously improved motor function and significantly enhanced functional recovery after 3 weeks. The engrafted cells were detected in the ipsilateral brain, most intensively in the peri-infarct area, expressing neuronal and glial markers. On the other hand, high-dose MSC-treated animals showed transient motor recovery from one to 3 weeks and then gradually



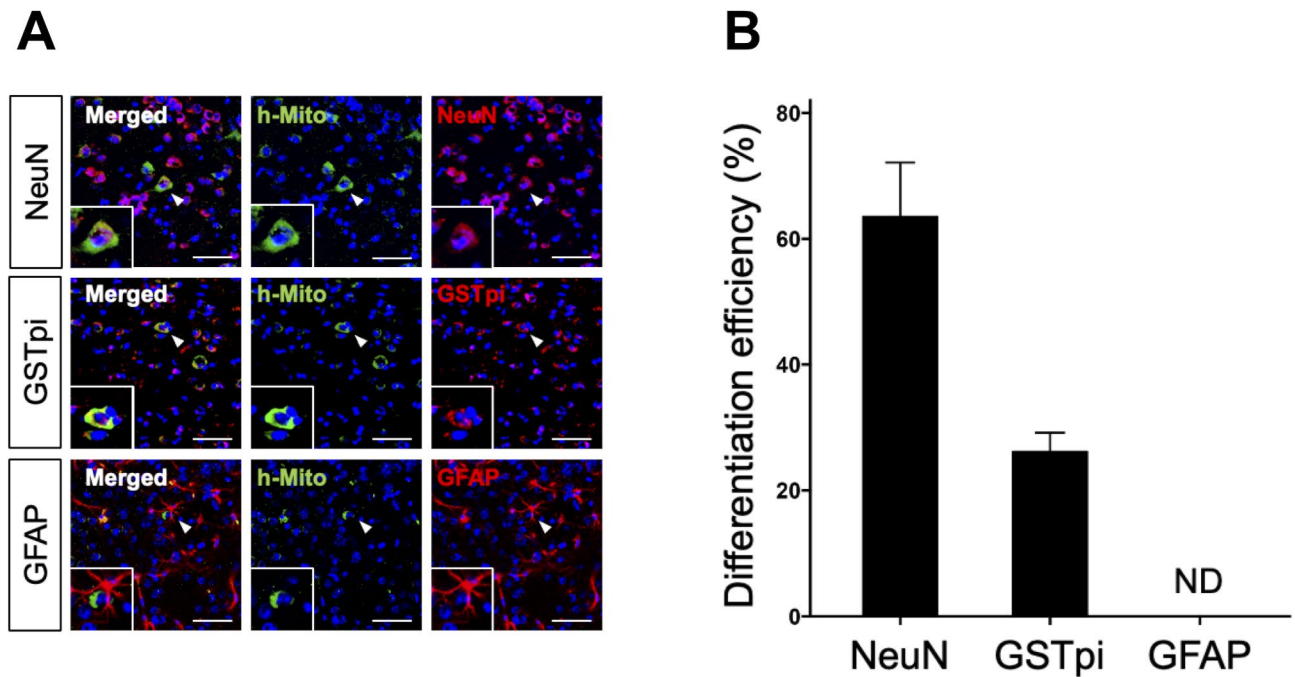


**Fig. 4.** Differentiation of Muse cells in the infarct brain. (A) On multi-color fluorescence immunohistochemistry, the human-mitochondria-positive Muse cells were doubly positive for NeuN (red, upper; arrowhead) and GSTpi (red, middle; arrowhead), but not for GFAP (red, lower; arrowhead). The white square shows the magnified images of the cell indicated by the arrowheads. Scale bar = 50 μm. h-Mito, human-mitochondria. (B) A bar graph shows the percentages of NeuN-, GSTpi-, and GFAP-positive cells in human-mitochondria-positive cells in the Muse group. ND, not detected.

deteriorated after that (Fig. 1). At the end point of 77 days, the motor function recovery in the Muse group was the best among the groups.

The difference in the pattern of functional recovery between the Muse and high-dose MSC groups might be explained by their biological characteristics; Muse cells are known to home to the post-infarct area by sensing S1P produced by damaged cells, differentiate into neural cells that comprise the tissue by phagocytosing apoptotic cells, replace the apoptotic neurons and glial cells with healthy functional cells to repair the tissues<sup>13,14</sup>. Not only did Muse cells replenish neuronal cells, but they were also reported to extend the neurites that reconstruct neuronal circuits to deliver functional recovery<sup>13,14</sup>. Since the neuronal circuit reconstruction takes time, the functional recovery became significant after several weeks after local injection and intravenous injection of Muse cell treatment in rodent stroke models<sup>13,14</sup>. This might partly explain the reason why the rotarod score improved after 3 weeks but not in the earlier period in the Muse group in this study. Furthermore, allogenic and xenogenic Muse cells are not rejected for an extended period without immunosuppressants due to specific immunotolerance mechanisms, including the expression of HLA-G, relevant to the immunotolerance mechanism in the placenta<sup>37</sup>. Allogenic Muse cells were shown to survive in the post-infarct heart tissue as cardiac cells for six months, and xenogenic human Muse cells were incorporated as human-collagen 7 and -collagen 18 producing epidermal cells in the mouse epidermolysis bullosa model, both without immunosuppressant<sup>10,38</sup>. A double-blind, placebo-controlled, randomized clinical trial for subacute cerebral infarction showed that a single intravenous injection of HLA-mismatched donor Muse cells without immunosuppressant showed safety and the maintenance of the statistically meaningful functional recovery until 52 weeks<sup>17</sup>. In this manner, intranasally administered Muse cells structurally and functionally recovered the MCAO model mice in this study.

MSCs are heterogeneous cell populations that secrete neurotrophic, anti-inflammatory, anti-apoptotic, and anti-fibrosis factors, serving tissue protection effects in the damaged brain<sup>39,40</sup>. However, those effects do not persist for a long time because most MSCs disappear from the body by several weeks after administration<sup>13</sup>. Previous studies showed that about half of the engrafted MSCs into the infarct brain expressed the mRNA for brain-derived neurotrophic factor (BDNF) and nerve growth factor (NGF) at 14 days after transplantation; however, their survival percent rapidly decreased thereafter<sup>41</sup>. Similar phenomenon has been observed when the neural stem cells are transplanted into the infarct brain, where they could not survive over one week after transplantation<sup>42</sup>. These reports may explain the transient effects observed in the high-dose MSC group within 2 to 3 weeks in this study.

Muse cells are contained in MSCs as several percent<sup>5–8</sup>. When MSCs are separated into several % SSEA-3(+) Muse cells and 97–98% SSEA-3(-) non-Muse MSCs, they showed clear differences; Muse cells can differentiate into ectodermal-, mesodermal-, and endodermal-lineages both by cytokine induction and phagocytosis-induced differentiation systems, migrate to the damaged site by sensing a universal tissue damage signal S1P, and a long term immunotolerance is possible for the allograft and xenograft Muse cells without immunosuppressant; while

non-Muse MSCs differentiated only into osteocytes-, chondrocytes- and adipocytes-lineages and not to other lineages, SDF-1-CXCR4 and HGFC-Met systems, not relevant to damaged tissues, are the main axes that control non-Muse cell migration, and do not establish long-lasting immunotolerance but escape from immunological attack by the production of immunosuppressive factors for a short time period<sup>43</sup>. Taken together, early and transient functional recovery observed in the high-dose MSC group may result from the transient tissue protection effects mainly exerted by the non-Muse MSCs.

Despite the high-dose MSC group contained the same number of Muse cells as the Muse group, the motor function recovery was confined to one to 3 weeks with a lower extent than that in the Muse group and was not sustained thereafter (Fig. 1). Consistently, the number of human mitochondria-positive cells was low in the high-dose MSC group than in the Muse group in the host brain ( $p < 0.001$ ; Fig. 4). The reason why Muse cells contained in the high-dose MSC group could not deliver a functional recovery comparable to that in the Muse group could be explained by the presence of a large number of non-Muse MSCs. 97–98% of MSCs is occupied by non-Muse MSCs, who has a strong anti-inflammation effect that leads to the suppression of S1P production in the damaged tissue<sup>44</sup>. This effect might have disturbed the homing ability of Muse cells to damage tissue, leading to the abrogation of the beneficial function of Muse cells. Therefore, there are reasonable reasons to administer purified Muse cells rather than bulk MSCs.

Although the usefulness of intranasal administration of various drugs has been widely recognized for decades<sup>45</sup>, intranasal transplantation for cell therapy is a relatively novel strategy for the treatment of central nervous system disorders. Recently, the efficacy of intranasal transplantation of MSCs has been examined in animal models of neonatal hypoxic-ischemic stroke, ischemic stroke, and intracerebral hemorrhage<sup>31,32,46</sup>. Donega et al.<sup>46</sup> intranasally administered MSCs into nine-day-old mice with carotid artery occlusion and hypoxia. When given 3 or 10 days after injury, intranasally administered MSCs reached the lesion site within 24 h, leading to the improvement of cognitive and sensorimotor functions. Chau et al.<sup>31</sup> intranasally administered MSCs into the mice model of ischemic stroke at 3, 4, 5, and 6 days, and such repeatedly treated animals showed significant recovery in sensorimotor function, local cerebral blood flow, and the number of neural cells in the peri-infarct area. Sun et al.<sup>32</sup> intranasally administered MSCs pre-treated with hypoxic preconditioning into the mice model of intracerebral hemorrhage at 3 and 7 days after the onset. MSC-treated mice revealed functional recovery from 14 days to 21 days after onset of intracerebral hemorrhage. Intranasally delivered MSCs migrated to peri-injury regions and produced factors such as BDNF, GDNF, and VEGF that have positive effects on neuroprotection and neurogenesis<sup>32</sup>. On the other hand, Parajuli et al.<sup>47</sup> administrated induced pluripotent stem cell-derived human microglia into the murine brain intranasally and found that human microglia were able to migrate through the cribriform plate to different regions of the brain, proliferate, and become the dominant microglia for at least 60 days with exogenous human cytokine.

Several hypotheses have been proposed regarding the pathways through which drugs and cells delivered intranasally reach the brain, including the olfactory, trigeminal, and perivascular pathways<sup>48</sup>. The olfactory route is divided into the parenchymal and cerebrospinal fluid (CSF) branches. The former may partially be associated with the rostral migratory stream, the major track by which neural progenitor cells migrate from the subventricular zone of the lateral ventricle to the olfactory bulb<sup>49</sup>. The latter passes through the cerebrospinal fluid, which was suggested as one of the possible routes of intranasally delivered drugs into the brain. The trigeminal route is also suggested to be consisted of at least two branches. One of which crosses the cribriform plate into the parenchyma, where it diverges to the rostral and caudal parts of the brain. The second branch projects from the nasal mucosa to the trigeminal ganglion, from where the transplanted cells are further distributed to the forebrain, olfactory bulb, and caudal parts of the brain, including the brain stem and the cerebellum<sup>50</sup>. The importance of the perivascular route as a conduit of cell trafficking is further emphasized by a recent study demonstrating the migration of olfactory bulb neuroblasts along blood vessels<sup>51</sup>. The migrating cells are suggested to associate with the vasculature in the granule cell layer of the olfactory bulb and use them as a scaffold for their migration through an interaction with the extracellular matrix and perivascular astrocyte end feet<sup>52</sup>. Using such migration routes, the intranasally administrated cells are known to quickly migrate to brain parenchyma within 1.5 h after the administration<sup>33</sup>.

The present study has some limitations. First, since we conducted only one kind of behavioral test, the interpretation of the effectiveness of intranasal transplantation of Muse cells is limited. Other neurological functional assessments, such as spatial memory, are required. Second, nasal administration is non-invasive, and multiple doses are feasible, particularly in clinics. Multiple doses through the nasal cavities might be of interest, particularly for older patients with ischemic stroke<sup>31</sup>. Further studies are warranted to elucidate the effects of intranasal transplantation of Muse cells on cognitive function and to assess the therapeutic effects of multiple doses of Muse cells through the nasal cavity for ischemic stroke.

## Conclusion

Muse cells migrated into the ipsilateral side of the brain after intranasal administration, integrated into the post-infarct area as cells positive for neuronal and glial cell markers, and delivered an improvement in functional recovery after ischemic stroke. Intranasal administration is a less invasive strategy for cell therapy and thus would be a feasible treatment for elders in clinical situations.

## Data availability

The data supporting the findings of this study are available from the corresponding author upon reasonable request from any investigator.

Received: 27 January 2025; Accepted: 28 March 2025

## References

- Goyal, M. et al. Endovascular thrombectomy after large-vessel ischaemic stroke: a meta-analysis of individual patient data from five randomised trials. *Lancet (Lond. Engl.)* **387**, 1723–1731. [https://doi.org/10.1016/s0140-6736\(16\)00163-x](https://doi.org/10.1016/s0140-6736(16)00163-x) (2016).
- Abe, K. et al. Stem cell therapy for cerebral ischemia: from basic science to clinical applications. *J. Cereb. Blood Flow. Metabolism: Official J. Int. Soc. Cereb. Blood Flow. Metabolism.* **32**, 1317–1331. <https://doi.org/10.1038/jcbfm.2011.187> (2012).
- Bliss, T. M., Andres, R. H. & Steinberg, G. K. Optimizing the success of cell transplantation therapy for stroke. *Neurobiol. Dis.* **37**, 275–283. <https://doi.org/10.1016/j.nbd.2009.10.003> (2010).
- Chen, J. et al. Therapeutic benefit of intravenous administration of bone marrow stromal cells after cerebral ischemia in rats. *Stroke* **32**, 1005–1011. <https://doi.org/10.1161/01.str.32.4.1005> (2001).
- Kuroda, Y. et al. Unique multipotent cells in adult human mesenchymal cell populations. *Proc. Natl. Acad. Sci. U S A.* **107**, 8639–8643. <https://doi.org/10.1073/pnas.0911647107> (2010).
- Wakao, S. et al. Multilineage-differentiating stress-enduring (Muse) cells are a primary source of induced pluripotent stem cells in human fibroblasts. *Proc. Natl. Acad. Sci. U S A* **108**, 9875–9880. <https://doi.org/10.1073/pnas.1100816108> (2011).
- Sato, T. et al. A novel type of stem cells double-positive for SSEA-3 and CD45 in human peripheral blood. *Cell. Transpl.* **29**, 963689720923574. <https://doi.org/10.1177/0963689720923574> (2020).
- Kushida, Y. et al. Human post-implantation blastocyst-like characteristics of muse cells isolated from human umbilical cord. *Cell. Mol. Life Sci.* **81**, 297. <https://doi.org/10.1007/s00018-024-05339-4> (2024).
- Ogawa, E. et al. Naive pluripotent-like characteristics of non-tumorigenic muse cells isolated from human amniotic membrane. *Sci. Rep.* **12**, 17222. <https://doi.org/10.1038/s41598-022-22282-1> (2022).
- Yamada, Y. et al. S1P-S1PR2 axis mediates homing of muse cells into damaged heart for Long-Lasting tissue repair and functional recovery after acute myocardial infarction. *Circ. Res.* **122**, 1069–1083. <https://doi.org/10.1161/CIRCRESAHA.117.311648> (2018).
- Wakao, S. et al. Phagocytosing differentiated cell-fragments is a novel mechanism for controlling somatic stem cell differentiation within a short time frame. *Cell. Mol. Life Sci.* **79**, 542. <https://doi.org/10.1007/s00018-022-04555-0> (2022).
- Kushida, Y., Wakao, S. & Dezawa, M. Muse cells are endogenous reparative stem cells. *Adv. Exp. Med. Biol.* **1103**, 43–68. [https://doi.org/10.1007/978-4-431-56847-6\\_3](https://doi.org/10.1007/978-4-431-56847-6_3) (2018).
- Yamauchi, T. et al. Therapeutic effects of human multilineage-differentiating stress enduring (MUSE) cell transplantation into infarct brain of mice. *PLoS One* **10**, e0116009. <https://doi.org/10.1371/journal.pone.0116009> (2015).
- Uchida, H. et al. Human muse cells reconstruct neuronal circuitry in subacute lacunar stroke model. *Stroke* **48**, 428–435. <https://doi.org/10.1161/strokeaha.116.014950> (2017).
- Noda, T., Nishigaki, K. & Minatoguchi, S. Safety and efficacy of human muse cell-based product for acute myocardial infarction in a first-in-human trial. *Circ. J.* **84**, 1189–1192. <https://doi.org/10.1253/circj.CJ-20-0307> (2020).
- Fujita, Y. et al. Intravenous allogeneic multilineage-differentiating stress-enduring cells in adults with dystrophic epidermolysis Bullosa: a phase 1/2 open-label study. *J. Eur. Acad. Dermatol. Venereol.: JEADV.* **35**, e528–e531. <https://doi.org/10.1111/jdv.17201> (2021).
- Niizuma, K. et al. Randomized placebo-controlled trial of CL2020, an allogeneic muse cell-based product, in subacute ischemic stroke. *J. Cereb. Blood Flow. Metabolism: Official J. Int. Soc. Cereb. Blood Flow. Metabolism.* **43**, 2029–2039. <https://doi.org/10.1177/0271678x231202594> (2023).
- Yamashita, T. et al. Safety and clinical effects of a muse cell-based product in patients with amyotrophic lateral sclerosis: results of a phase 2 clinical trial. *Cell Transplant.* **32**, 9636897231214370. <https://doi.org/10.1177/09636897231214370> (2023).
- Sato, Y. et al. Safety and tolerability of a muse cell-based product in neonatal hypoxic-ischemic encephalopathy with therapeutic hypothermia (SHIELD trial). *Stem Cells Transl. Med.* **13**, 1053–1066. <https://doi.org/10.1093/stcltm/szae071> (2024).
- Koda, M. et al. Safety and feasibility of intravenous administration of a single dose of allogeneic-Muse cells to treat human cervical traumatic spinal cord injury: a clinical trial. *Stem Cell Res. Ther.* **15**, 259. <https://doi.org/10.1186/s13287-024-03842-w> (2024).
- Li, Y. et al. Intrastriatal transplantation of bone marrow nonhematopoietic cells improves functional recovery after stroke in adult mice. *J. Cereb. Blood Flow. Metabolism: Official J. Int. Soc. Cereb. Blood Flow. Metabolism.* **20**, 1311–1319. <https://doi.org/10.1097/0004647-200009000-00006> (2000).
- Osana, T. et al. Therapeutic effects of intra-arterial delivery of bone marrow stromal cells in traumatic brain injury of rats—in vivo cell tracking study by near-infrared fluorescence imaging. *Neurosurgery* **70**, 435–444. <https://doi.org/10.1227/NEU.0b013e318230a795> (2012). discussion 444.
- Chen, J. et al. Intravenous bone marrow stromal cell therapy reduces apoptosis and promotes endogenous cell proliferation after stroke in female rat. *J. Neurosci. Res.* **73**, 778–786. <https://doi.org/10.1002/jnr.10691> (2003).
- Li, Y. et al. Human marrow stromal cell therapy for stroke in rat: neurotrophins and functional recovery. *Neurology* **59**, 514–523. <https://doi.org/10.1212/wnl.59.4.514> (2002).
- Shen, L. H. et al. Therapeutic benefit of bone marrow stromal cells administered 1 month after stroke. *J. Cereb. Blood Flow. Metabolism: Official J. Int. Soc. Cereb. Blood Flow. Metabolism* **27**, 6–13. <https://doi.org/10.1038/sj.jcbfm.9600311> (2007).
- Shen, L. H. et al. One-year follow-up after bone marrow stromal cell treatment in middle-aged female rats with stroke. *Stroke* **38**, 2150–2156. <https://doi.org/10.1161/strokeaha.106.481218> (2007).
- Fischer, U. M. et al. Pulmonary passage is a major obstacle for intravenous stem cell delivery: the pulmonary first-pass effect. *Stem Cells Dev.* **18**, 683–692. <https://doi.org/10.1089/scd.2008.0253> (2009).
- Detante, O. et al. Intravenous administration of 99mTc-HMPAO-labeled human mesenchymal stem cells after stroke: in vivo imaging and biodistribution. *Cell. Transpl.* **18**, 1369–1379. <https://doi.org/10.3727/096368909x474230> (2009).
- Danielyan, L. et al. Intranasal delivery of cells to the brain. *Eur. J. Cell Biol.* **88**, 315–324. <https://doi.org/10.1016/j.ejcb.2009.02.001> (2009).
- Donega, V. et al. Assessment of long-term safety and efficacy of intranasal mesenchymal stem cell treatment for neonatal brain injury in the mouse. *Pediatr. Res.* **78**, 520–526. <https://doi.org/10.1038/pr.2015.145> (2015).
- Chau, M. J. et al. Delayed and repeated intranasal delivery of bone marrow stromal cells increases regeneration and functional recovery after ischemic stroke in mice. *BMC Neurosci.* **19**, 20. <https://doi.org/10.1186/s12868-018-0418-z> (2018).
- Sun, J. et al. Intranasal delivery of hypoxia-preconditioned bone marrow-derived mesenchymal stem cells enhanced regenerative effects after intracerebral hemorrhagic stroke in mice. *Exp. Neurol.* **272**, 78–87. <https://doi.org/10.1016/j.expneurol.2015.03.011> (2015).
- Wei, N. et al. Delayed intranasal delivery of hypoxic-preconditioned bone marrow mesenchymal stem cells enhanced cell homing and therapeutic benefits after ischemic stroke in mice. *Cell. Transpl.* **22**, 977–991. <https://doi.org/10.3727/096368912x657251> (2013).
- Lee, J. et al. Migration and differentiation of nuclear fluorescence-labeled bone marrow stromal cells after transplantation into cerebral infarct and spinal cord injury in mice. *Neuropathology* **23**, 169–180. <https://doi.org/10.1046/j.1440-1789.2003.00496.x> (2003).
- Kuroda, Y. et al. Isolation, culture and evaluation of multilineage-differentiating stress-enduring (Muse) cells. *Nat. Protoc.* **8**, 1391–1415. <https://doi.org/10.1038/nprot.2013.076> (2013).



36. Tamura, Y. et al. Intracellular translocation of glutathione S-transferase Pi during oligodendrocyte differentiation in adult rat cerebral cortex in vivo. *Neuroscience* **148**, 535–540. <https://doi.org/10.1016/j.neuroscience.2007.06.026> (2007).
37. Kuroda, Y., Oguma, Y., Hall, K. & Dezawa, M. Endogenous reparative pluripotent muse cells with a unique immune privilege system: hint at a new strategy for controlling acute and chronic inflammation. *Front. Pharmacol.* **13**, 1027961. <https://doi.org/10.3389/fphar.2022.1027961> (2022).
38. Fujita, Y. et al. Injection of muse cells as a potential therapeutic approach for epidermolysis bullosa. *J. Invest. Dermatol.* **141**, 198–202 e196. <https://doi.org/10.1016/j.jid.2020.05.092> (2021).
39. Wang, L. et al. Neural progenitor cells treated with EPO induce angiogenesis through the production of VEGF. *J. Cereb. Blood Flow. Metabolism: Official J. Int. Soc. Cereb. Blood Flow. Metabolism* **28**, 1361–1368. <https://doi.org/10.1038/jcbfm.2008.32> (2008).
40. Kuroda, S. Bone marrow stromal cell transplantation for ischemic stroke—its multi-functional feature. *Acta Neurobiol. Exp. (Wars.)* **73**, 57–65. <https://doi.org/10.55782/ane-2013-1921> (2013).
41. Shichinohe, H. et al. Bone marrow stromal cells rescue ischemic brain by trophic effects and phenotypic change toward neural cells. *Neurorehabil. Neural Repair.* **29**, 80–89. <https://doi.org/10.1177/1545968314525856> (2015).
42. Kelly, S. et al. Transplanted human fetal neural stem cells survive, migrate, and differentiate in ischemic rat cerebral cortex. *Proc. Natl. Acad. Sci. U.S.A.* **101**, 11839–11844. <https://doi.org/10.1073/pnas.0404474101> (2004).
43. Minatoguchi, S. et al. Donor muse cell treatment without HLA-Matching tests and immunosuppressant treatment. *Stem Cells Transl. Med.* **13**, 532–545. <https://doi.org/10.1093/stcltm/szae018> (2024).
44. Takahashi, M. et al. Structural reconstruction of mouse acute aortic dissection by intravenously administered human muse cells without immunosuppression. *Commun. Med. (Lond.)* **4**, 174. <https://doi.org/10.1038/s43856-024-00597-6> (2024).
45. Lochhead, J. J. & Thorne, R. G. Intranasal delivery of biologics to the central nervous system. *Adv. Drug Deliv. Rev.* **64**, 614–628. <https://doi.org/10.1016/j.addr.2011.11.002> (2012).
46. Donega, V. et al. Intranasal mesenchymal stem cell treatment for neonatal brain damage: long-term cognitive and sensorimotor improvement. *PLoS One* **8**, e51253. <https://doi.org/10.1371/journal.pone.0051253> (2013).
47. Parajuli, B. et al. Transnasal transplantation of human induced pluripotent stem cell-derived microglia to the brain of immunocompetent mice. *Glia* **69**, 2332–2348. <https://doi.org/10.1002/glia.23985> (2021).
48. Li, G., Bonamici, N., Dey, M., Lesniak, M. S. & Balyasnikova, I. V. Intranasal delivery of stem cell-based therapies for the treatment of brain malignancies. *Expert Opin. Drug Deliv.* **15**, 163–172. <https://doi.org/10.1080/17425247.2018.1378642> (2018).
49. Luskin, M. B. Restricted proliferation and migration of postnatally generated neurons derived from the forebrain subventricular zone. *Neuron* **11**, 173–189. [https://doi.org/10.1016/0896-6273\(93\)90281-u](https://doi.org/10.1016/0896-6273(93)90281-u) (1993).
50. Crowe, T. P., Greenlee, M. H. W., Kanthasamy, A. G. & Hsu, W. H. Mechanism of intranasal drug delivery directly to the brain. *Life Sci.* **195**, 44–52. <https://doi.org/10.1016/j.lfs.2017.12.025> (2018).
51. Lochhead, J. J., Wolak, D. J., Pizzo, M. E. & Thorne, R. G. Rapid transport within cerebral perivascular spaces underlies widespread tracer distribution in the brain after intranasal administration. *J. Cereb. Blood Flow. Metabolism: Official J. Int. Soc. Cereb. Blood Flow. Metabolism* **35**, 371–381. <https://doi.org/10.1038/jcbfm.2014.215> (2015).
52. Bovetti, S. et al. Blood vessels form a scaffold for neuroblast migration in the adult olfactory bulb. *J. Neurosci.* **27**, 5976–5980. <https://doi.org/10.1523/jneurosci.0678-07.2007> (2007).

## Author contributions

S. Y. and K. S. conducted animal experiments. S. Y. and Y. K. conducted data analysis. S. Y. and Y. K. prepared Figures. Y. K. and Y. O. conducted cell preparation and histological analysis. S. Y. wrote the main manuscript text. S. W., M. D., and S. K. supervised the study. All authors reviewed the manuscript.

## Funding

This work was supported by JSPS KAKENHI Grant Number JP23K08515.

## Competing interests

The authors declare no competing interests.

## Additional information

**Correspondence** and requests for materials should be addressed to S.Y., M.D. or S.K.

**Reprints and permissions information** is available at [www.nature.com/reprints](http://www.nature.com/reprints).

**Publisher's note** Springer Nature remains neutral with regard to jurisdictional claims in published maps and institutional affiliations.

**Open Access** This article is licensed under a Creative Commons Attribution-NonCommercial-NoDerivatives 4.0 International License, which permits any non-commercial use, sharing, distribution and reproduction in any medium or format, as long as you give appropriate credit to the original author(s) and the source, provide a link to the Creative Commons licence, and indicate if you modified the licensed material. You do not have permission under this licence to share adapted material derived from this article or parts of it. The images or other third party material in this article are included in the article's Creative Commons licence, unless indicated otherwise in a credit line to the material. If material is not included in the article's Creative Commons licence and your intended use is not permitted by statutory regulation or exceeds the permitted use, you will need to obtain permission directly from the copyright holder. To view a copy of this licence, visit <http://creativecommons.org/licenses/by-nc-nd/4.0/>.

© The Author(s) 2025